AIP | Applied Physics Letters

Thermo-electric effect in a nano-sized crossed Permalloy/Cu junction under high bias current

Congpu Mu, Shaojie Hu, Jianbo Wang, and Takashi Kimura

Citation: Applied Physics Letters **103**, 132408 (2013); doi: 10.1063/1.4822330
View online: http://dx.doi.org/10.1063/1.4822330
View Table of Contents: http://scitation.aip.org/content/aip/journal/apl/103/13?ver=pdfcov
Published by the AIP Publishing

Thermo-electric effect in a nano-sized crossed Permalloy/Cu junction under high bias current

Congpu Mu,[1,2] Shaojie Hu,[1,3] Jianbo Wang,[2] and Takashi Kimura[1,4,5,a)]
[1]*Advanced Electronics Research Division, INAMORI Frontier Research Center, Kyushu University, 744 Motooka, Fukuoka 819-0395, Japan*
[2]*Institute of Applied Magnetics, Key Laboratory for Magnetism and Magnetic Materials of the Ministry of Education, Lanzhou University, Lanzhou 730000, People's Republic of China*
[3]*Graduate School of Information Science and Electrical Engineering, Kyushu University, 744 Motooka, Fukuoka 819-0395, Japan*
[4]*Department of Physics, Kyushu University, 6-10-1 Hakozaki, Fukuoka 812-8581, Japan*
[5]*CREST, Japan Science and Technology Agency, Sanbancho, Tokyo 102-0075, Japan*

(Received 15 June 2013; accepted 10 September 2013; published online 25 September 2013)

We show that the difference in the Seebeck coefficients between two voltage probes produces an additional electric signal in the local resistance measurement of the submicron-sized junction. This is because the temperature increase at the junction induced by the Joule heating produces unnegligible Seebeck voltage in addition to the Ohmic voltage. In nanostructured systems, since the temperature variation becomes quite high under the high-bias current, the Seebeck voltage dominates the detected electrical voltage. This provides a consistent description for unusual bias-current dependences of the differential resistance in nano-sized metallic junction systems. © *2013 AIP Publishing LLC*. [http://dx.doi.org/10.1063/1.4822330]

Electrical transport measurement is a powerful means for understanding the physical properties of metallic and semiconductor materials. Recent developments of nanofabrications provide multi-terminal nano-sized electrical probes, which enable to detect the transport properties in nanostructured materials and nano-sized elements selectively and sensitively.[1–5] In such systems, since the sample dimension is comparable or less than the characteristic lengths such as phase coherence length and spin-diffusion length, various intriguing phenomenon have been reported.[6,7] Novel transport properties such as spin-dependent and ballistic transports have also reported recently.[8–11] Indeed, the giant and tunnel magneto resistance effects are widely utilized as high sensitive magnetic sensor in the practical applications.[12,13]

In nanostructured systems, thermally induced phenomenon becomes important in addition to the transport phenomenon because the temperature of the small element is easily modified by extrinsic effects.[14] Especially, the interaction between the spin and heat currents, which is known as the emerging field of spincaloritronics,[15,16] is creating a renewed interests because of possible application for spin manipulations. Moreover, novel spin-related thermal properties, such as spin and spin-dependent Seebeck and Peltier effects, have been reported in unique spincaloritronic systems.[17–20] Therefore, thermal transports in ferromagnetic/nonmagnetic hybrid structures have been intensively investigated very recently.[21–23] However, there are still numerous controversial issues and un-conventional phenomena in such nanostructured thermoelectric effects.[24,25] For proper understanding these nontrivial thermal transport properties, first of all, the interplay between the charge and heat currents plays an important role. Especially, relatively large Seebeck coefficients in the ferromagnetic transition metals as well as their anisotropies may induce a large undesired electrical signal in addition to the tiny spin-related signal.[26] Indeed, the back ground signal much larger than the spin related signal is found to be induced in the nonlocal voltage probe under the electrical spin injection.[27,28] Moreover, the structural changes due to the migration effects may have to be considered as the possible origin for such unconventional phenomena.[29,30] Here, we focus on the influence of the heat current in a ferromagnetic/nonmagnetic junction. We show that the thermoelectric effect is dominant contribution of the electrical voltage even in a local configuration.

We have fabricated a laterally configured ferromagnetic/nonmagnetic metal junction. Figure 1 shows a scanning electron microscope (SEM) image of the fabricated device together with its schematic illustration. Here, Permalloy (Py) wires, 100 nm in width and 40 nm in thickness, have been fabricated by electron-beam lithography with a conventional lift-off technique on a thermally oxidized Si substrate. Then, a Cu strip, 300 nm in width and 180 nm in thickness, has been fabricated by repeating the same lift-off process. Here, in order to obtain highly transparent interface, the surface of the Py was cleaned by low-voltage Ar ion milling prior to the Cu deposition. The transparency and cleanliness have been confirmed by the lateral spin transports, such as local and nonlocal spin valve measurements.[28] The representative nonlocal spin signal of the present device measured at room temperature is shown in Fig. 1(a). We have also fabricated a simple Cu cross with the same lateral dimension, for a comparison,

To study the thermo-electric effect induced by the current, we mainly study the bias current dependence of the resistance at the corner of the cross-shaped wire, whose probe configuration is shown in Fig. 1(b). Here, the current is swept from −1.5 mA to +1.5 mA. The maximum current densities for the Py, Cu, and the Py/Cu junctions are 3.75×10^{11} A/m^2, 2.78×10^{10} A/m^2, and 5.10×10^{11} A/m^2, respectively. So, the current density becomes the highest value in the Py wire.

a)kimura@ifrc.kyushu-u.ac.jp

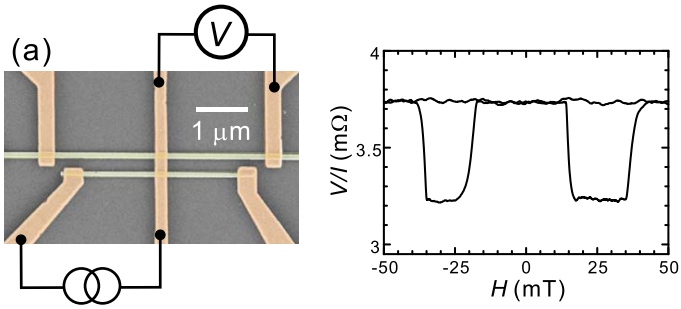

FIG. 1. (a) SEM image of the fabricated sample consisting of laterally configured ferromagnetic/nonmagnetic junctions together with the representative nonlocal spin signal observed at room temperature. (b) Definition of the corner resistance and the expected current distribution at the corner.

However, the value is lower the critical value for the migration in Py.[31] When the cross consists of a polycrystalline homogeneous metal, the electrical voltage is mainly induced by the Ohmic resistance because the mean free path of the polycrystalline metallic wire is a few ten nanometer, which is much shorter than the lateral dimension of the device.[32] As shown in Fig. 1(b), when the charge current flows from the left to the bottom electrode, the positive voltage difference is observed between the top and right electrodes because of the Ohmic resistance. By increasing the bias current flowing in the corner, the voltage linearly increases because of the Ohm's law. In addition, when the cross consists of a junction, the interface resistance is additionally superimposed on the Ohmic resistance. It should be noted that the sign of the voltage contribution from the interface resistance is opposite to that from the Ohmic resistance, as shown in Fig. 1(b). Moreover, the thermo-electric effects are also induced in the vicinity of the junction and modified the electric resistance via Joule heating and/or Peltier effect.

First, we evaluate the bias-current dependence of the corner resistance for the homogeneous Cu cross. As seen in Fig. 2(a), the voltage increases almost linearly with the dc bias current because of the Ohm's law. However, if we carefully check the dependence, a small deviation from the linear dependence is observed under the high bias current.

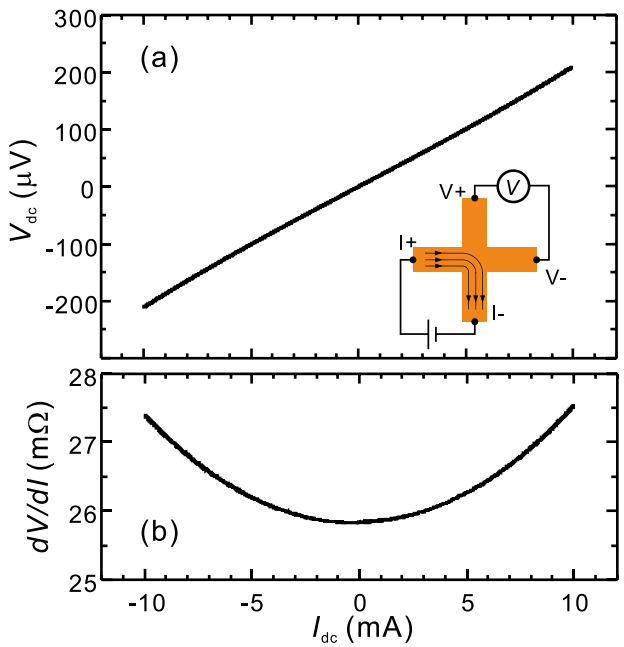

FIG. 2. (a) Dependence voltage as a function of the DC bias current in the homogeneous Cu cross. (b) DC bias current dependences of the differential resistance defined by dV/dI.

To show this nonlinear behavior more clearly, the resistance defined by dV/dI is plotted in Fig. 2(b). A parabolic dependence is clearly observed, meaning that the temperature of the measured region is increased by the Joule heating.[33]

We then measure the bias-current dependence of the corner resistance for the Cu/Py junction. As shown in Fig. 3(a), the bias-dependence of the voltage shows the quite different features from that in the Cu cross. Especially, it is surprising that the voltage becomes negative under the positive bias current above +1.4 mA. One of the possible origins is the increase of the interface resistance because the contribution of the interface resistance is negative in the present measurement configuration. However, it is impossible to explain the parabolic enhancement of the voltage under the negative bias current. The possibilities of the migration effects can also be excluded by the experimental fact that the observed characteristics are reversible changes.[29,30]

In order to understand the parabolic increase of the voltage, we consider the Seebeck effect induced by the heating at the junction. As mentioned in Fig. 1, under the high bias current, the temperature at the junction increases because of the Joule heating. When the temperature at the junction is locally heated, the electrical voltage is induced by the Seebeck voltage in the Py/Cu junction. The induced voltage is given by the following equation:[27]

$$V = (S_{\mathrm{Py}} - S_{\mathrm{Cu}})\Delta T. \tag{1}$$

Here, S_{Py} and S_{Cu} are the Seebeck coefficients for the Py and Cu, respectively. By assuming that the temperature change ΔT is proportional to I^2, the parabolic dependence observed in Fig. 3(a) is well reproduced. As another important feature of the Seebeck voltage, we measure the probe configuration dependence of the induced voltage. According to Eq. (1), the sign of the induced voltage should be reversed by interchange V+ and V− terminals. Since the voltage due to the Ohmic resistance should satisfy the reciprocal relationship, we should interchange I+ and I− in another probe configuration. Therefore, we measure the bias current dependence of the corner resistance with the reversed probe configuration. As shown in Fig. 3(b), we observe the reversed parabolic dependence, supporting Eq. (1).

To confirm our expectation more clearly, we define the average voltage V_{avg} and the voltage difference V_{dif} as follows:

$$V_{\mathrm{avg}} = \frac{V_{\mathrm{A}} + V_{\mathrm{B}}}{2}, \tag{2}$$

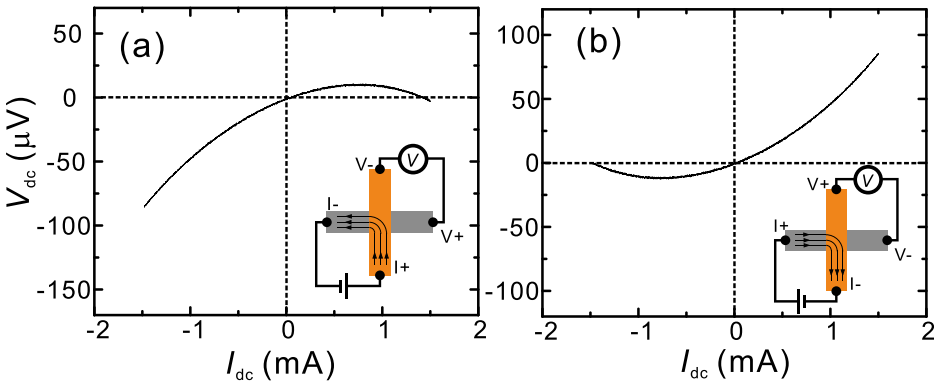

FIG. 3. (a) Induced voltage at the corner as a function of the DC bias current in the submicron-scale Cu/Py junction when the current flows from Cu to Py (configuration A). (b) Induced voltage at the corner as a function of the DC bias current when the current flows from Py to Cu (configuration B). The insets show the probe configuration for each corner resistance measurement.

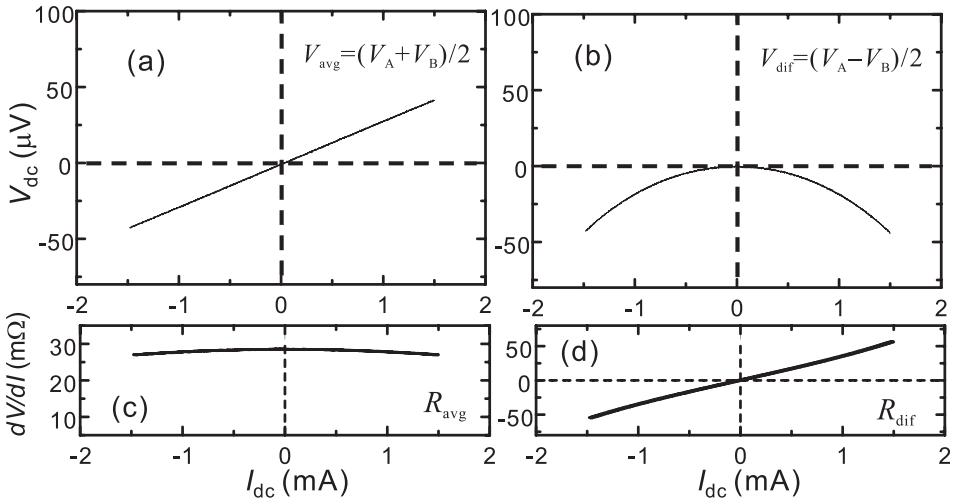

FIG. 4. DC bias current dependences of (a) V_{Avg} and (b) V_{Dif}. DC bias current dependences of (c) the differential resistance defined by dV_{Avg}/dI and (d) that defined by dV_{Dif}/dI.

$$V_{dif} = \frac{V_A - V_B}{2}. \tag{3}$$

Here, V_A and V_B are the observed voltages in the configuration of Figs. 3(a) and 3(b), respectively. As mentioned before, the sign of the Seebeck voltage depends on the probe configuration while that of the Ohmic voltage does not depend on the probe configuration. Therefore, V_{avg} and V_{dif} give the Ohmic and Seebeck voltages, respectively. Figures 4(a) and 4(b) show, respectively, V_{avg} and V_{dif} as a function of the dc bias current. V_{avg} behaves similarly to Fig. 2, indicating that the V_{avg} is produced by the Ohmic resistance of the corner. In Fig. 4(b), we also confirm a perfect parabolic dependence without any background. This clearly supports that the voltage is induced by the Seebeck effect combined with the Joule heating. The differential resistances R_{avg} and R_{dif} defined by dV_{avg}/dI and dV_{dif}/dI, respectively, are also plotted in Figs. 4(c) and 4(d). dV_{avg}/dI shows the reversed parabolic dependence due to the negative contribution of the interface resistance. A small linear component, which produces the horizontal shift of the parabolic curve, is explained by the Peltier effect in the Py/Cu junction.

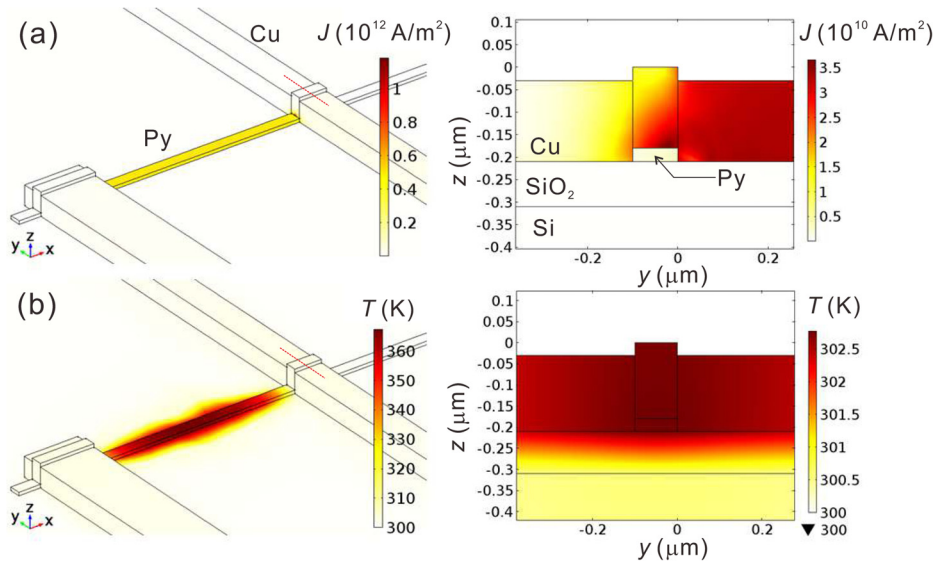

FIG. 5. Numerically simulated three-dimensional spatial distributions for (a) the current density and (b) the temperature in the vicinity of the Py/Cu junction under the bias current of 1.5 mA. In the right-hand sand, the cross-sectional images focusing on the junction are plotted.

dV_{dif}/dI increases almost linearly, but includes a slight deviation from the linear dependence. This may be because the Seebeck coefficient under the high bias current is slightly modified by the Joule heating.

Finally, in order to show the reliability of our scenario more quantitatively, we have numerically calculated the spatial distributions of the current and the temperature in the vicinity of the Py/Cu junction. Figures 5(a) and 5(b) show the three dimensional color plots for the calculated current density and the temperature, respectively. Here, 1.5 mA dc current flows from the Py wire into the Cu wire. As shown in Fig. 5(a), the current distribution around the junction is quite inhomogeneous because of the large conductivity of the Cu wire with the bias electric field. On the other hand, the temperature distribution is homogeneous around the junction. This means that one dimensional model can be applied for the analysis of the thermoelectric effect. From Fig. 5(b), we can evaluate the temperature increase ΔT at the junction is approximately 2.5 K under the bias current of 1.5 mA. Since the Seebeck coefficients for the Cu and Py are 1.6 μV/K and $-20\,\mu$V/K,[17,18] the observed voltage $-45\,\mu$V is quantitatively explained by the present scenario.

Thus, the Seebeck effect in the voltage probe produces a significant measurable electrical voltage. Surprisingly, we showed that, in the nano-sized Py/Cu junction, it is much larger than the Ohmic voltage produced by the local current flow. A similar situation occurs in a current-perpendicular-to-plane giant magnetoresistive structure with a nano-sized metallic junction.[33] Therefore, unusual behaviors of the bias-current dependence of the electrical resistance[34,35] may be explained by taking into account the Seebeck voltage in the voltage probe.

This work was partially supported by CANON Foundation, NEDO, and CREST. The authors (C.M. and S.H.) acknowledge the China Scholarship Council for Young Scientists.

[1]J. Nygard, D. Cobden, and P. Lindelhof, Nature (London) **408**, 342 (2000).
[2]A. K. Geim and K. S. Novoselov, Nature Mater. **6**(3), 183–191 (2007).
[3]M. Tsutsui, M. Taniguchi, and T. Kawai, Nat. Commun. **1**, 138 (2010).
[4]T. Ono, H. Miyajima, K. Shigeto, and T. Shinjo, Appl. Phys. Lett. **72**, 1116 (1998).
[5]M. M. Deshmukh and D. C. Ralph, Phys. Rev. Lett. **89**, 266803 (2002).
[6]K. Tsukagoshi, B. Alphenaar, and H. Ago, Nature **401**, 572–574 (1999).
[7]K. Yakushiji, F. Ernult, H. Imamura, K. Yamane, S. Mitani, K. Takanashi, S. Takahashi, S. Maekawa, and H. Fujimori, Nature Mater. **4**, 57 (2005).
[8]H. D. Chopra and S. Z. Hua, Phys. Rev. B **66**, 020403R (2002).
[9]U. Ebels, A. Radulescu, Y. Henry, L. Piraux, and K. Ounadjela, Phys. Rev. Lett. **84**, 983 (2000).
[10]F. J. Jedema, A. T. Filip, and B. J. van Wees, Nature (London) **410**, 345 (2001).
[11]T. Kimura, Y. Otani, T. Sato, S. Takahashi, and S. Maekawa, Phys. Rev. Lett. **98**, 156601 (2007).
[12]S. S. P. Parkin, C. Kaiser, A. Panchula, P. M. Rice, B. Hughes, M. Samant, and S.-H. Yang, Nature Mater. **3**, 862 (2004).
[13]S. Yuasa, T. Nagahama, A. Fukushima, Y. Suzuki, and K. Ando, Nature Mater. **3**, 868 (2004).
[14]D. G. Cahill, W. K. Ford, K. E. Goodson, G. D. Mahan, A. Majumdar, H. J. Maris, R. Merlin, and S. R. Phillpot, J. Appl. Phys. **93**, 793 (2003).
[15]G. E. W. Bauer, A. H. MacDonald, and S. Maekawa, Solid State Commun. **150**, 459 (2010).
[16]G. E. W. Bauer, E. Saitoh, and B. J. van Wees, Nature Mater. **11**, 391 (2012).
[17]K. Uchida, S. Takahashi, K. Harii, J. Ieda, W. Koshibae, K. Ando, S. Maekawa, and E. Saitoh, Nature **455**, 778 (2008).
[18]A. Slachter, F. L. Bakker, J. P. Adam, and B. J. van Wees, Nat. Phys. **6**, 879 (2010).
[19]J. Flipse, F. L. Bakker, A. Slachter, F. K. Dejene and B. J. van Wees, Nat. Nanotechnol. **7**, 166 (2012).
[20]J. C. Le Breton, S. Sharma, H. Saito, S. Yuasa, and R. Jansen, Nature (London) **475**, 82 (2011).
[21]F. Giazotto, T. Heikkila, A. Luukanen, A. Savin, and J. Pekola, Rev. Mod. Phys. **78**, 217 (2006).
[22]S. Petit-Watelot, R. Otxoa, M. Manfrini, W. Van Roy, L. Lagae, J. V. Kim, and T. Devolder, Phys. Rev. Lett. **109**, 267205 (2012).
[23]S. Krompiewski, Phys. Rev. B **80**, 075433 (2009).
[24]J. Sinova, Nature Mater. **9**, 880 (2010).
[25]S. Y. Huang, X. Fan, D. Qu, Y. P. Chen, W. G. Wang, J. Wu, T. Y. Chen, J. Q. Xiao, and C. L. Chien, Phys. Rev. Lett. **109**, 107204 (2012).
[26]A. Asamitsu, Y. Moritomo, and Y. Tokura, Phys. Rev. B **53**, R2952 (1996).
[27]L. Bakker, A. Slachter, J.-P. Adam, and B. J. van Wees, Phys. Rev. Lett. **105**, 136601 (2010).
[28]S. J. Hu and T. Kimura, Phys. Rev. B **87**, 014424 (2013).
[29]P. Kumar, M. G. Krishna, and A. K. Bhattacharya, Int. J. Nanosci. **7**, 255–261 (2008).
[30]P. Kumar and K. Sangeeth, Nanosci. Nanotechnol. Lett. **1**, 194–198 (2009).
[31]A. Yamaguchi, S. Nasu, H. Tanigawa, T. Ono, K. Miyake, K. Mibu, and T. Shinjo, Appl. Phys. Lett. **86**, 012511 (2005).
[32]G. Mihajlovic, J. E. Pearson, M. A. Garcia, S. D. Bader, and A. Hoffmann, Phys. Rev. Lett. **103**, 166601 (2009).
[33]J. Katine, F. Albert, R. Buhrman, E. Myers, and D. Ralph, Phys. Rev. Lett. **84**, 3149 (2000).
[34]A. Fukushima, K. Yagami, A. A. Tulapukkar, Y. Suzuki, H. Kubota, A. Yamamoto, and S. Yuasa, Jpn. J. Appl. Phys., Part 2 **44**, L12 (2005).
[35]A. Sugihara, M. Kodzuka, K. Yakushiji, H. Kubota, S. Yuasa, A. Yamamoto, K. Ando, K. Takanashi, T. Ohkubo, K. Hono, and A. Fukushima, Appl. Phys. Express **3**, 065204 (2010).